Title

Quantitative Multiplex Substrate Profiling of Peptidases by Mass Spectrometry*

Journal

Molecular & Cellular Proteomics, 18(5)

ISSN

1535-9476

Authors

Lapek, John D

Jiang, Zhenze

Wozniak, Jacob M

et al.

Publication Date

2019-05-01

DOI

10.1074/mcp.tir118.001099

Quantitative Multiplex Substrate Profiling of Peptidases by Mass Spectrometry

Authors

John D. Lapek Jr., Zhenze Jiang, Jacob M. Wozniak, Elena Arutyunova, Steven C Wang, M. Joanne Lemieux, David J. Gonzalez, and Anthony J. O'Donoghue

Correspondence

djgonzalez@ucsd.edu;
ajodonoghue@ucsd.edu

In Brief

Peptidases play essential roles in numerous biological pathways. It is important to characterize their specificities in order to fully understand their functions. Here, we combined tandem mass tags (TMTs) with an established peptide cleavage assay to yield quantitative Multiplex Substrate Profiling by Mass Spectrometry (qMSP-MS). TMT labeling together with enzyme kinetics modeling greatly improves throughput, reproducibility and quantification accuracy of the assay. Additionally, this method is capable of characterizing specificities of both purified peptidases and complex biological samples containing multiple peptidases.

Graphical Abstract

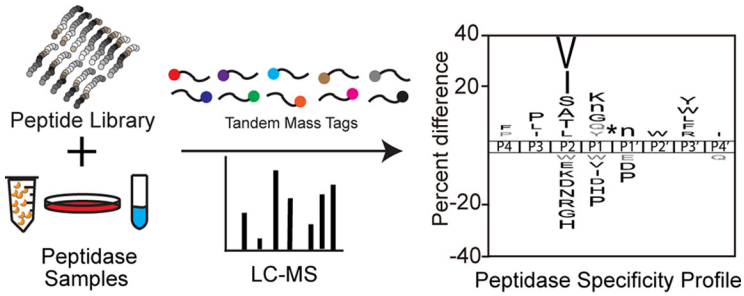

Highlights

- Quantitative substrate profiling method for characterizing peptidase specificity.
- Applicable to both purified peptidases and peptidases in complex biological samples.
- TMT labeling improves throughput, accuracy and reproducibility of the assay.
- Design of fluorescent probes to monitor peptidase activity based on substrate data.

Lapek et al., 2019, Molecular & Cellular Proteomics *18*, 968–981

https://doi.org/10.1074/mcp.TIR118.001099

Quantitative Multiplex Substrate Profiling of Peptidases by Mass Spectrometry*[S]

John D. Lapek Jr.‡§‡‡, Zhenze Jiang§¶‡‡, Jacob M. Wozniak‡§, Elena Arutyunova‖, Steven C Wang§**, M. Joanne Lemieux‖, David J. Gonzalez‡§§§, and Anthony J. O'Donoghue§¶¶

Proteolysis is an integral component of life and has been implicated in many disease processes. To improve our understanding of peptidase function, it is imperative to develop tools to uncover substrate specificity and cleavage efficiency. Here, we combine the quantitative power of tandem mass tags (TMTs) with an established peptide cleavage assay to yield quantitative Multiplex Substrate Profiling by Mass Spectrometry (qMSP-MS). This assay was validated with papain, a well-characterized cysteine peptidase, to generate cleavage efficiency values for hydrolysis of 275 unique peptide bonds in parallel. To demonstrate the breath of this assay, we show that qMSP-MS can uncover the substrate specificity of minimally characterized intramembrane rhomboid peptidases, as well as define hundreds of proteolytic activities in complex biological samples, including secretions from lung cancer cell lines. Importantly, our qMSP-MS library uses synthetic peptides whose termini are unmodified, allowing us to characterize not only endo- but also exo-peptidase activity. Each cleaved peptide sequence can be ranked by turnover rate, and the amino acid sequence of the best substrates can be used for designing fluorescent reporter substrates. Discovery of peptide substrates that are selectively cleaved by peptidases which are active at the site of disease highlights the potential for qMSP-MS to guide the development of peptidase-activating drugs for cancer and infectious disease. ***Molecular & Cellular Proteomics 18: 968–981, 2019. DOI: 10.1074/mcp.TIR118.001099.***

Peptidases play an important role in maintaining cellular health. These enzymes generally catalyze irreversible reactions and thus it is imperative that their activity is tightly controlled. Unregulated proteolysis results in protein and peptide substrates being cleaved at faster rates or at unusual sites. In human disease, an increase in proteolytic activity may be because of up-regulation or mis-localization of peptidases or down-regulation of endogenous inhibitors (1–3). During infection, invading microbes or host immune response can also cause an increase in proteolytic activity. Irrespective of the source of the activity, it is important to understand the substrate preference of disease associated peptidases as it will facilitate the development of tools that can selectively monitor, enhance, or inhibit their activities. Many assays have been developed to reveal the substrate specificity of peptidases, including the use of synthetic fluorogenic peptides (4–7), bacterial and phage displayed peptides (8, 9), and proteome derived proteins and peptides (10–14). Peptide display technologies can generate vast numbers of diverse substrate sequences, however mapping the exact cleavage locus is not trivial and requires downstream mutagenesis or mass spectrometry studies. Technologies that use cellular proteins or peptides as substrates generally require enrichment steps to separate cleaved from uncleaved proteins (15, 16). In addition, the concentration of each substrate in the protein extract can differ greatly, making it difficult to compare the cleavage rate among substrates. These technologies are semi-quantitative and limited in their ability to distinguish the cleavage efficiency of each substrate. Fluorescent methods, such as positional scanning synthetic combinatorial libraries (4, 17, 18), are generally more quantitative and can take advantage of natural and nonnatural amino acids. However, these substrates lack extended amino acid sequence on the carboxy-terminal side of the scissile bond, and the location of the fluorophore adjacent to the scissile bond can impede enzyme-substrate binding interactions.

Our group previously developed a peptide degradation assay that uses tandem mass spectrometry to identify cleavage products within an equimolar mixture of tetradecapeptide substrates (19). These peptides were rationally designed such that all possible neighbor and near-neighbor amino acid pairs are present in the library and hydrolysis of any of the 2964 peptide bonds can be detected by tandem mass spectrom-

From the ‡Department of Pharmacology, University of California San Diego, 9500 Gilman Drive La Jolla, California 92093; §Skaggs School of Pharmacy and Pharmaceutical Sciences, University of California San Diego, 9500 Gilman Drive La Jolla, California 92093; ¶Department of Chemistry and Biochemistry, University of California San Diego, 9500 Gilman Drive La Jolla, California 92093; ‖Department of Biochemistry, Faculty of Medicine and Dentistry, Membrane Protein Disease Research Group, University of Alberta, Edmonton, Alberta T6G 2R3, Canada; **Division of Biological Sciences, University of California, San Diego, 9500, Gilman Drive, La Jolla, California 92093

Received September 19, 2018, and in revised form, December 31, 2018
Published, MCP Papers in Press, January 31, 2019, DOI 10.1074/mcp.TIR118.001099

etry. In addition, every substrate has a unique dipeptide sequence on the amino and C termini to facilitate the characterization of amino- and carboxy-peptidase substrate specificity. The amino acid sequences of the synthetic substrates are distinct from endogenous proteins and peptides; therefore, when complex biological samples are assayed with this library, cleaved products are easily discriminated from endogenous peptides. This assay has been used to uncover the substrate specificity profile of enzymes from every peptidase family, and the data generated from these assays has guided the development of optimized fluorescent reporters (20, 21), peptide inhibitors (22, 23), activity-based probes (24), therapeutic peptides (25), and activity-based biomarkers (26). All peptide substrates are present at equimolar concentration and this assay identifies cleavage products that appear at defined time-intervals following addition of enzyme.

In this study, we used isobaric tandem mass tags (TMT)[1] (27, 28) to quantify all cleaved and uncleaved peptides within the tetradecapeptide substrate library following addition of a peptidase or a complex sample containing multiple peptidases. The reaction was incubated for up to 20 h and different TMTs were used to label each of the assay time-points. Changes in peptide abundance were quantified and proteolytic kinetic constants were calculated (Fig. 1). In addition to providing quantification, TMT labeling can also minimize experimental and instrument variation while allowing us to gain crucial temporal information. This combination greatly improves the reproducibility and accuracy, while also allowing for a reduction in instrument time by 10-fold. We have named this approach Quantitative Multiplex Substrate Profiling by Mass Spectrometry (qMSP-MS).

First, we used a well characterized peptidase, papain, to validate the qMSP-MS assay. In addition, the substrate specificity of two integral membrane peptidases were characterized, and a fluorescent reporter was developed based on the preferred peptide substrate, which can be used for high-throughput biochemical assays. Finally, we analyzed lung cancer cell secretions using our workflow and found that they generally produced exopeptidases that can degrade the peptides at the amino and C termini. These results highlight the potential of applying quantitative mass spectrometry to proteolytic assays which can lead to the development of novel therapeutic delivery systems for important human diseases.

EXPERIMENTAL PROCEDURES

Experimental Design and Statistical Rationale—A total of 144 samples were analyzed in this study using the qMSP-MS assay, corresponding to 12 different peptidase samples; papain, PsAarA, HiGlpG, *Aspergillus phoenicis* extract and secretions from 8 lung cancer cell lines (supplemental Table S1). For each peptidase reaction, time points were taken after 0.25, 1, 4, and 20 h of incubation. Papain, *Aspergillus phoenicis* extract, PsAarA and HiGlpG samples were assayed in triplicate enzyme reactions whereas triplicate lung cancer secretion samples were generated from three separate culture flasks. A total of 27 samples were analyzed by proteomics corresponding to secretions from 8 lung cancer cell lines and *Aspergillus phoenicis* extract in triplicate. Replicate lung cancer cell lines were labeled with different TMTs and assayed via mass spectrometry. The *Aspergillus phoenicis* extract was not labeled with TMT. Significance was assessed by ANOVA and Student's *t* test; variance was assessed by an F-test to ensure the correct statistical assumptions were used. q-values of $q \leq 0.05$ were considered significant.

Expression and Purification of Rhomboid Proteins—The purification of all rhomboid proteins was like the previous report (29). Briefly, rhomboid genes were cloned into pBAD-Myc/HisA plasmid (Invitrogen, Carlsbad, CA), having a C-terminal tobacco etch virus (TEV) peptidase cleavage site, Myc-epitope and His6-tag, were expressed in TOP10 *E. coli* cells. The protein was induced with 0.002% w/v arabinose and expressed at 24 °C for 8 h in LB media. The cells were harvested, resuspended in 50 mM Tris-HCl pH 8.0, 150 mM NaCl and lysed under high pressure using an EmulsiFlex-C3 (Avestin, Ottawa, Ontario, Canada). The membranes were isolated by ultracentrifugation at 95,800 × *g* for 2 h, solubilized in 50 mM Tris-HCl pH 8.0, 300 mM NaCl, 10 mM imidazole, 20% glycerol, 1% (w/v) DDM and applied onto a Ni-NTA column (Qiagen, Hilden, Germany). The proteins were eluted with 250–500 mM of imidazole, 50 mM Tris-HCl pH 8.0, 300 mM NaCl, 20% glycerol, 0.1% DDM. From 1L of cell culture, purified protein yield was 1–2 mg for PsAarA and 2–3 mg for HiGlpG. The His-tag was removed by TEV peptidase (1 mg per 100 mg of protein, overnight, 16 °C) and a subsequent Ni-NTA column was performed to remove uncleaved protein and TEV peptidase. The flow-through was collected and concentrated using 30,000 MWCO concentrators (Millipore, Burlington, MA). The protein samples (supplemental Fig. S1) were flash-frozen and stored at −80 °C before analysis.

Collection of Lung Cancer Secretions—Lung cancer cell lines BEN, H520, H2228, H460, H661, DMS273, and SHP77 were cultured in RPMI 1640 (Corning, Corning, NY) supplemented with 10% fetal bovine serum (Corning) and 100 U/ml penicillin-streptomycin (HyClone, Logan, UT). The cell line H1944 was cultured in RPMI 1640 supplemented with 10% fetal bovine serum, 1.5 g/L $NaHCO_3$ (HyClone), 4.5 g/L glucose, 10 mM HEPES (GE Healthcare Life Sciences, Chicago, IL), 1 mM sodium pyruvate (HyClone) and 100 U/ml penicillin-streptomycin (HyClone). All cells were maintained at 37 °C in an atmosphere of 5% CO_2 and grown to ~80% confluence in triplicate T-175 flasks. Culture media was removed, and cells were washed twice with Dulbecco's PBS (Thermo, Waltham, MA) and twice with RPMI 1640. Cells were then incubated with serum-free RPMI 1640 for 24 h. The conditioned media was removed, filtered (0.22 μm) and subsequently buffer-exchanged and concentrated into Dulbecco's PBS using an Amicon Ultra centrifugal filter (EMD Millipore, Burlington, MA) with 10-kDa cutoff. Protein concentration was determined by BCA assay (Thermo).

Protein Identification of Aspergillus Phoenicis (Aspph) Extract—Two hundred micrograms of *Aspph* extract (Sigma, St. Louis, MO, P2143) was incubated with 1% sodium deoxycholate (Thermo), 10 mM tris(2-carboxyethl)phosphine (Sigma), 40 mM chloroacetamide (Sigma), and 100 mM Tris pH 8.0, (Research Products International, Mt. Prospect, IL) at 90 °C for 10 min. Samples were cooled to room temperature and diluted 2× in 100 mM Tris (pH 8.0). Trypsin (sequencing grade, Promega V5113, Madison, WI) was added at 1:50 trypsin/total protein for digestion overnight at 37 °C. Reactions were

[1] The abbreviations used are: TMT, tandem mass tag; qMSP-MS, quantitative multiplex substrate profiling by mass spectrometry; *Aspph*, *Aspergillus phoenicis*; PsAarA, *Providencia stuartii* AarA; HiGlpG, *Haemophilus influenza* GlpG; NSCLC, non-small cell lung cancer; SCLC, small cell lung cancer; ANOVA, analysis of variance; Mca, 7-methoxycoumarin-4-acetic acid; DNP, 2,4-dinitrophenol; AMC, 7-amino-4-methylcoumarin.

quenched by adding 10% TFA to bring the pH down to ~2 and desalted using C18 LTS tips (Rainin, Oakland, CA). Two micrograms of the extracted peptides were analyzed on a Q Exactive Mass Spectrometer (Thermo) equipped with an Ultimate 3000 HPLC (Thermo). Peptides were separated by reverse phase chromatography on a C_{18} column (1.7 μm bead size, 75 μm × 20 cm, heated to 65 °C) at a flow rate of 300 nL/min using a 56-min linear gradient from 4% B to 17% B followed by a 20-min gradient from 17% B to 25% B, with solvent A: 0.1% formic acid (Thermo) in water and solvent B: 0.1% formic acid in acetonitrile (Thermo). Survey scans were recorded over a 350–1200 *m/z* range at 35,000 resolution at 200 *m/z*. MS/MS was performed in data-dependent acquisition mode with HCD fragmentation (28 normalized collision energy) on the 20 most intense precursor ions at 17,500 resolution at 200 *m/z*. Data was processed using PEAKS 8.5 (Bioinformatics Solutions Inc.). MS^2 data were searched against *Aspergillus phoenicis* proteome and annotated by InterPro (JGI Project ID: 1020378). Fixed modifications of carbamidomethylation of cysteines (+57.02146 Da), variable modification of acetylation of protein N termini (+42.0106) and oxidation of methionine (+15.99492 Da) were specified. A precursor tolerance of 20 ppm and 0.01 Da for MS^2 fragments was defined. Data were filtered to 1% peptide and protein level false discovery rates with the target-decoy strategy.

Protein Identification and Quantification in Lung Cancer Secretions—Secreted proteins were denatured in a buffer containing 75 mM NaCl (Sigma), 3% sodium dodecyl sulfate (SDS, Thermo), 1 mM NaF (Sigma), 1 mM β-glycerophosphate (Sigma), 1 mM sodium orthovanadate (Sigma), 10 mM sodium pyrophosphate (Sigma), 1 mM phenylmethylsulfonyl fluoride (Sigma), and 1× Complete Mini EDTA free peptidase inhibitors (Roche, Indianapolis, IN) in 50 mM HEPES (Sigma), pH 8.5 (30). Insoluble debris was pelleted by centrifugation for 5 min at 18,000 × *g* at 22 °C. Supernatants were transferred into fresh tubes, and an equal volume of 8 M urea (Thermo) in 50 mM HEPES, pH 8.5 was added to each sample. Samples were then vortexed briefly and sonicated for 5 min in a sonicating water bath to maximize protein denaturation.

Proteins were reduced and alkylated as previously described (31). Proteins were then precipitated via a methanol-chloroform procedure (32). Precipitated proteins were resolubilized in 300 μl of 1 M urea (Thermo) in 50 mM HEPES (Thermo), pH 8.5. Solubility was aided through vortexing, sonicating, and manual grinding. Proteins were then digested in a two-stage process. First, 3 μg of LysC (Wako 129–02541, Osaka, Japan) was added to each sample and allowed to incubate overnight at room temperature. Next, 3 μg of trypsin (Promega V5113) was added, and samples were allowed to digest for 6 h at 37 °C. Digestion was quenched by addition of trifluoroacetic acid (TFA, Pierce, Waltham, MA). Peptides were desalted with C18 Sep-Paks (Waters, Milford, MA) as previously described (33). Peptide concentration was determined with a PepQuant Assay (Thermo), and peptides were aliquoted into 50 μg portions which were dried under vacuum and stored at −80 °C until they were labeled with TMT reagents.

Peptides were labeled with 10-plex TMT reagents (Thermo) (27, 28) as previously described (34). TMTs were reconstituted at a concentration of 20 μg/μl in dry acetonitrile (Sigma). Dried peptides were reconstituted in 30% dry acetonitrile in 200 mM HEPES, pH 8.5, and 8 μl of the appropriate TMT reagent was added to peptides. Reagents 126 and 131 were used to bridge among mass spectrometry runs (35) whereas the remaining TMT reagents were used to label samples as listed in supplemental Table S2. Labeling was carried out for one hour at room temperature and was quenched by adding 9 μl of 5% hydroxylamine (Sigma). Samples were acidified with 50 μl of 1% TFA then pooled into appropriate 10-plex TMT samples, with pooled standard samples labeled with 126 and 131. Pooled 10-plex samples were desalted with C18 Sep-Paks.

Samples were separated into eight fractions by basic pH reverse-phase chromatography using spin columns (Pierce). Fractions were dried then reconstituted in 5% formic acid/5% acetonitrile and analyzed on an Orbitrap Fusion Tribrid Mass Spectrometer (Thermo) equipped with an EASY-nLC 1000 (Thermo) for identification and quantitation. MS^2/MS^3 analysis for identification was carried out with chromatographic and mass spectrometry acquisition settings as previously defined (36, 37). Briefly, peptides were separated on a 100 μm ID × 30 cm home-pulled home-packed column (0.5 cm C_4 5 μm, 100Å and 29.5 cm C_{18} 1.8 μm, 120Å). A linear gradient from 11 to 30% Acetonitrile in 0.135% formic acid over 165 min at a flow rate of 300 nL/min with the column heated to 60 °C was used for separation. The mass spectrometer was operated in data dependent mode, with a survey scan across the mass to charge range of 500–1200 at 120,000 resolution in the Orbitrap. Automatic Gain Control (AGC) target was set to 5×10^5 with a max ion time of 100 ms. The s-lens was set at an RF of 60. Top speed mode was used to select the most abundant ions for MS^2/MS^3 in a 5 s experimental cycle. For MS^2 analysis, precursors were isolated with the quadrupole at a width of 0.5 *m/z*. CID normalized energy was 30% and fragments were detected in the ion trap at rapid scan rate. AGC was set to 1×10^4 with a max ion time of 35 ms. For MS^3 analysis, SPS was used with a maximum of 10 ions isolated for MS^3 analysis. These ions were fragmented with HCD at a normalized energy of 50% and detected in the Orbitrap at 60,000 resolution with a low mass of 110 *m/z*. AGC was set to 5×10^4 with a maximum ion time of 150 ms. MS^2 precursors were excluded in a range of 40 *m/z* below and 15 *m/z* above the MS^1 precursor. All data (MS^1, MS^2, MS^3) were centroided. Data were processed using Proteome Discoverer 2.1 (Thermo). MS^2 data were searched against Uniprot Human (05/11/2017) using the Sequest algorithm (38). A decoy search was also conducted with sequences in reverse order (39–41). A precursor tolerance of 50 ppm (42, 43) and 0.6 Da for MS^2 fragments was defined. Static modifications of TMT 10-plex tags on lysine and peptide N termini (+229.162932 Da) and carbamidomethylation of cysteines (+57.02146 Da) were specified. Variable oxidation of methionine (+15.99492 Da) was included in the search parameters as well. A maximum of two missed cleavages of trypsin was allowed. Data were filtered to 1% peptide and protein level false discovery rates with the target-decoy strategy through Percolator (44, 45). TMT reporter ion intensities were extracted from MS^3 spectra for quantitative analysis, and signal-to-noise ratios were used for quantitation. Spectra were filtered, summed, and normalized as previously described (35, 37).

Quantitative Multiplex Substrate Profiling—All qMSP-MS peptidase assays were performed in triplicate using an equimolar mixture of 228-synthetic tetradecapeptides. The final concentration of each peptide was 0.5 μM. Papain (3.3 μg/ml, Sigma, P4762) and *Aspph* extract (5 μg/ml, Sigma, P2143) were incubated with the peptide mixture in 20 mM Citrate-Phosphate buffer, pH 5.0, 100 mM NaCl, 1 mM $CaCl_2$ and 2 mM DTT. Membrane peptidases PsAarA (175 μg/ml) and HiGlpG (5 μg/ml) were assayed in 20 mM Citrate-Phosphate buffer, pH 6.0, 150 mM NaCl, 2 mM DTT, 20% Glycerol, 0.1% n-Dodecyl β-D-maltoside (DDM, Sigma). All lung cancer cell line secretions were assayed at 160 μg/ml of total protein in 20 mM Citrate-Phosphate buffer, pH 6.5, 100 mM NaCl, 1 mM $CaCl_2$, 2 mM DTT at 37 °C. For each assay, 10% of the reaction mixture was removed after 0.25, 1, 4, and 20 h of incubation. Enzyme activity was quenched by addition of GuHCl to a final concentration of 6.4 M and samples were immediately stored at −80 °C. Control samples consisted of enzyme incubated with 6.4 M GuHCl before addition of the peptide library. All samples were desalted with STAGE tips as previously described (46) and dried under vacuum.

Samples were reconstituted in 55 μl of 30% dry acetonitrile in 200 mM HEPES, pH 8.5 and assembled into groups of nine. 5 μl from each sample was removed and combined with samples from within the group (45 μl total in each tube + 5 μl 30% Dry acetonitrile in 200 mM HEPES, pH 8.5). A unique TMT reagent was used to label peptides in each tube as outlined in supplemental Table S3. The tube containing a mixture of samples was labeled with TMT-131 and used to generate bridge channels for inter-run normalization as described previously (35). Labeled samples were combined into appropriate 10-plex experiments and desalted with Sep-Paks. 10-plex experiments were dried and stored at −80 °C until mass spectrometry analysis. Samples were reconstituted in 8 μl of 5% formic acid in 5% acetonitrile and analyzed on an Orbitrap Lumos Tribrid Mass Spectrometer (Thermo) equipped with an EASY-nLC 1000 (Thermo) with 3 μl of sample analyzed for each 10-plex. Acquisition parameters were the same as those outlined above for lung cancer secretion proteomics. Data were processed using Proteome Discoverer 2.1 (Thermo) as outlined above with the exception that MS^2 data were searched against the 228 synthetic peptides library (supplemental Data S4) with no enzyme digestion specified and a decoy search was conducted with peptide sequences in reverse order (39–41). Data were filtered to 1% peptide level false discovery rates with the target-decoy strategy.

qMSP-MS Data Analysis—Proteolytic progress of each peptide was modeled by performing nonlinear least-squares regression to pseudo-first-order enzymatic kinetics: $Y = (\text{plateau-}Y_0) \times (1\text{-exp}(-t \times k_{cat}/K_m \times [E_0])) + Y_0$, where E_0 is the total enzyme concentration. Proteolytic efficiency was reported as k_{cat}/K_m for purified enzymes or k ($k = k_{cat}/K_m \times [E_0]$) for samples where the concentration of peptidase is unknown. Nonlinear fitting was performed on cleavage products only if peptides were detected in at least 2 of the 3 replicates and passed ANOVA test ($p < 0.05$). Cleaved peptides were clustered using Jenks natural breaks optimization and peptides in the group with highest proteolytic efficiencies were used to generate specificity profiles. Peptides in Group 2 are slowly formed cleavage products and proteolysis did not go to completion within the 20-hour assay time. The catalytic efficiency values for these peptides are less accurate as their progression curves are nonparabolic (linear) and cannot be well fitted with pseudo-first-order enzymatic kinetics. Peptidase activity correlates with peptidase stability and therefore it is likely that enzyme activity decreases during the 20-hour assay. For exopeptidases activities, a Student's *t* test was performed on cleavage products only if peptides were detected in at least 2 of the 3 replicates and were significant by ANOVA ($q < 0.05$). Peptides with a significant increase (*t* test $q < 0.05$) of at least 2-fold compared with controls were considered significantly increased and used to generate specificity profiles. Specificity profiles of peptidases were generated by iceLogo software (47) to visualize amino acid frequency surrounding the cleavage sites. Amino acids that were most frequently observed (above axis) and least frequently observed (below axis) from P4 to P4′ positions were illustrated ($p < 0.3$). Norleucine (Nle) was represented as 'n' in the reported profiles. Amino acids in opaque black text were statistically significant ($p < 0.05$).

Fluorescent Substrates Screening—Real-time fluorescence measurements were performed using a Synergy HTX Multi-Mode Microplate Reader (BioTek, Winooski, VT). PsAarA (175 μg/ml), HiGlpG (100 μg/ml) and HiGlpG S116A (100 μg/ml) were assayed with 5 μM of IQ1 (supplemental Table S4) in 20 mM Citrate-Phosphate, pH 6.0, 150 mM NaCl, 2 mM DTT, 20% Glycerol, 0.1% DDM. *Aspph* extract was assayed with 5 μM of IQ2 (supplemental Table S4) in 20 mM Citrate-Phosphate buffer, pH 5.0, 100 mM NaCl, 1 mM $CaCl_2$, 2 mM DTT, 1 mM EDTA (MP Biomedicals, Santa Ana, CA), 10 μM E64 (Sigma), 1 mM AEBSF (Tocris, Bristol, UK), and ± 1 μM Pepstatin (MP Biomedicals). Fluorescence was read at Ex/Em = 320/400 nm. The cleavage sites of the fluorescent substrates were mapped by mass spectrometry as described previously (48).

Lung cancer secretions (160 μg/ml) were mixed with 5 μM AMC substrates (supplemental Table S4) in 20 mM Citrate-Phosphate, pH 6.5, 100 mM NaCl, 1 mM $CaCl_2$, 2 mM DTT at 37 °C. Fluorescence was read at Ex/Em = 360/460 nm.

RESULTS

In our previous use of the substrate profiling assay, the peptide library was incubated with a peptidase and an aliquot of the reaction volume was removed at four time-intervals (T1 to T4), quenched with acid or denaturant, and analyzed by mass spectrometry. Although this assay has been successfully used to characterize many enzymes, the method is largely qualitative, where the time interval at which a cleavage product is first detected is correlated with cleavage efficiency. For example, a cleavage product discovered at T3 but absent in T1 and T2 was the result of a slower peptidase cleavage reaction than a product that is first detected at T1. In this study, peptide substrates are incubated with a peptidase, however, a unique TMT reagent is used to label cleaved and uncleaved peptides at each time-interval. Each labeled sample can then be combined into a single mass spectrometry experiment. This multiplex approach allows for accurate comparison of peptide abundance at each time point so that kinetic parameters such as k_{cat}/K_m can be directly calculated for the time dependent accumulation of each cleavage product (Fig. 1).

Validation of the Method Using Papain—To validate this method, we incubated the 228-peptide library with papain, a prototypical cysteine peptidase isolated from papaya fruit. This enzyme is homologous to all C1 family enzymes, the predominant cysteine peptidase found in microbes, plants, and animals (49). We detected cleavage at 275 of the 2,964 available peptide bonds within the tetradecapeptide library over the course of a 20-h incubation. The use of TMT in this assay allowed us to determine cleavage efficiency for the formation of every peptide product. The proteolytic constant k_{cat}/K_m was calculated from progress curves using the first-order kinetics formula: $Y = (\text{plateau-}Y_0) \times (1\text{-exp}(-t \times k_{cat}/K_m \times [E_0])) + Y_0$. The k_{cat}/K_m values ranged from 0.041 M^{-1} s^{-1} to 1.34×10^6 M^{-1} s^{-1} and were separated into 2 groups using the Jenks natural breaks algorithm (Fig. 2*A*). The progress curves for peptides in Group 1 consisting of the fastest cleaved substrates were parabolic and therefore the reaction was generally complete within 20 h (Fig. 2*B*). However, the progress curves for peptides in Group 2 (*e.g.* THATPGIHFVL*LRP) were linear and therefore these slow reactions were still progressing even after 20 h incubation (Fig. 2*B*). All cleaved products were matched to the parent 14-mer substrate in order to determine the cleavage location and identify the amino acids at both sides of the scissile bond. Papain hydrolyzed peptide bonds at each of the 13 sites within the substrates. However, cleavage of bonds between residues 1 to 3, and 12 to 14 occurred at lower frequency than at all other sites, indicating that papain is an

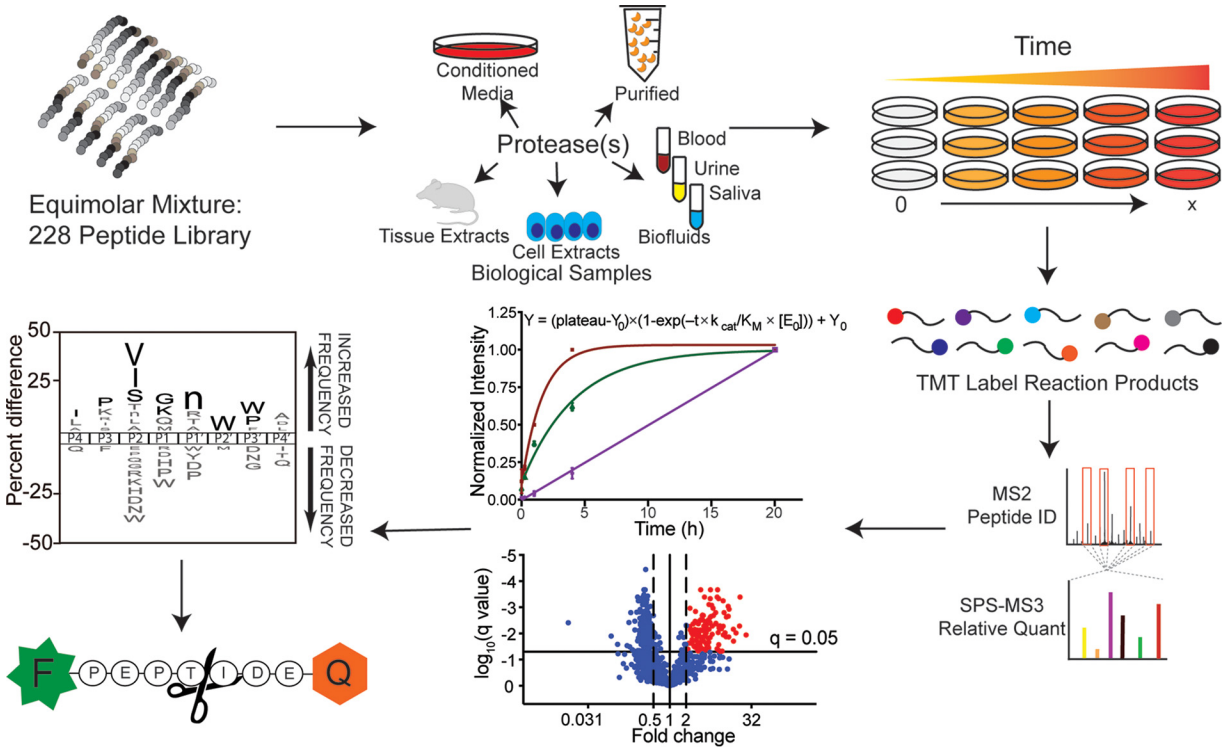

FIG. 1. **Workflow of qMSP-MS.** An equimolar mixture of 228 tetradecapeptides is incubated with a purified peptidase or a biological sample containing multiple peptidases. Aliquots of this assay are removed at multiple time intervals and the enzymes are inactivated with a denaturant. Quenched samples are labeled with specific TMTs and pooled before mass spectrometry analysis. Cleavage products are identified by MS/MS and quantified by TMT labels. Proteolytic progression curves or relative abundance changes of each cleavage product are calculated, and peptides are ranked by their proteolytic efficiency. Cleavage products with highest proteolytic efficiencies are selected to generate specificity profiles and design fluorescent substrates.

endopeptidase and has low preference for hydrolysis of bonds near the termini of peptides (Fig. 2*C*).

For each cleavage site found in this study, the amino acids in the P4 to P4′ positions were identified, and two distinct substrate specificity profiles were generated for papain representing the fastest and slowest substrates (Fig. 2*D*). The profile for the fastest substrates revealed that short aliphatic (Val, Ile, Leu, Ala) and hydroxylic (Ser, Thr) amino acids are preferred in the P2 position whereas Gly, Asn and charged amino acids such as Asp, Glu, Arg, Lys and His are not well tolerated. In the P3 position, papain has preference for Pro, Leu, Lys and Ile. Our results are consistent with previous studies (50, 51), and the P3 and P2 described here strongly correlate with the P3 (Spearman = 0.857) and P2 (Spearman = 0.755) specificity of papain when assayed with a combinatorial library of 160,000 fluorescent tetrapeptide substrates (52). In the P1 position, Lys, Gly, and Nle (norleucine; lowercase "n" in iceLogo) are favored whereas Pro, His, Asp, Ile, and Val are disfavored. This specificity weakly, but positively, correlates with the P1 preference found using the combinatorial library (Spearman = 0.44), most likely because of the position of the bulky fluorescent reporter molecule in the P1′ position, directly adjacent to the P1 amino acid. However, when internally quenched fluorescent substrates that do not have the fluorophore in the P1′ position were assayed with papain, Gly was found to be the preferred amino acid in the P1 position (53). On the prime side, Nle and Trp are preferred at P1′ and P2′ positions, respectively.

We next generated a specificity profile of papain using the amino acids surrounding the cleavage sites found in Group 2 (Fig. 2*E*). Peptides in Group 2 are cleaved slowly most likely because of one or more unfavorable amino acids present in the substrate sequence. In the P2 position, bulky hydrophobic amino acids, such as Tyr, Nle, Pro, and Phe are found instead of the small aliphatic and hydroxyl amino acids present in the Group 1 profile. Asp in the P1′ was the most favored amino acid in Group 2 but this residue is strongly disfavored in Group 1. Likewise, Gln in P4′ was favored in Group 2 and disfavored in Group 1. At other positions many of the same residues are common between Group 2 and Group 1. These data show that papain has broad specificity and the rate of substrate cleavage is primarily driven by the amino acid in the P2 position. In the absence of small aliphatic and hydroxyl amino acids, peptide hydrolysis does occur, but the rate is considerable slower than when these preferred amino acids are present.

Taken together, the qMSP-MS assay data allowed us to rank the papain cleavage events based on efficiency and

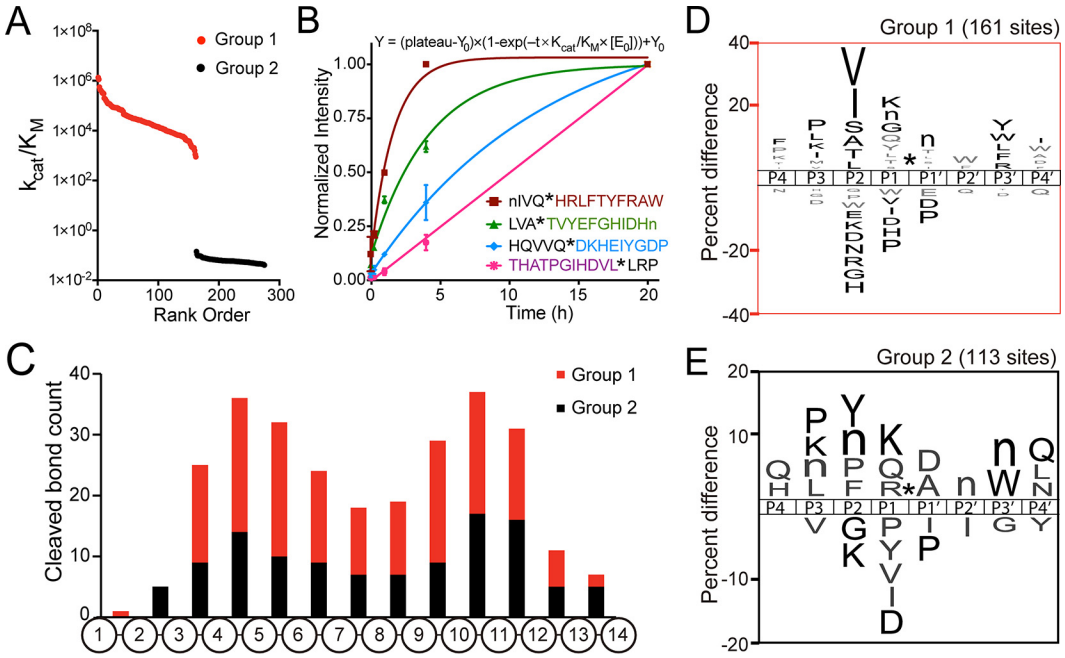

FIG. 2. **Quantitative multiplex substrate profiling of papain.** *A*, Proteolytic constant k_{cat}/K_m of each cleaved peptide was calculated, ranked, and clustered into Group 1 (red) and Group 2 (black). *B*, Progress curves for sample cleavage products from Group 1 (Brown, Green and Blue) and Group 2 (Pink). The sequence of the full-length substrate is shown, and the cleaved product quantified in this assay is colored. *C*, Distribution of Group 1 and 2 cleavage sites within 14-mer peptides. *D*, A frequency plot showing the P4 to P4′ specificity profile of substrates that a rapidly cleaved by papain (Group1). *E*, A frequency plot showing the P4 to P4′ specificity profile of substrates that a slowly cleaved by papain (Group 2). Lowercase "n" corresponds to norleucine and nongrayed residues have $p \leq 0.05$. Cleavage sites are indicated with *.

generate a substrate specificity profile corresponding to the bonds that are hydrolyzed rapidly compared with bonds that are slowly hydrolyzed. In addition, we show that papain is an endopeptidase and therefore preferentially hydrolyzes peptide bonds distal to the amino and C termini. These results demonstrate that qMSP-MS provides important kinetic information for peptidase mediated hydrolysis of peptide bonds.

Uncovering the Substrate Specificity of Membrane Embedded Intramembrane Peptidases—After validation of qMSP-MS assay with papain, we studied an intramembrane serine peptidase from *Providencia stuartii*, PsAarA. This enzyme has been defined as a bacterial rhomboid peptidase, and related enzymes are also found in mammalian cells. Rhomboid peptidases are known to control many cellular functions and play important roles in human diseases (54), however, few studies have been conducted to elucidate their substrate preferences. PsAarA is known to cleave the transmembrane protein TatA between a pair of Ala residues in the following sequence, IATAAFGS. Strisovsky and colleagues expressed more than 130 mutant variants of the TatA protein substrate that have different amino acid sequence surrounding the scissile bond and discovered that the P4, P1, and P2′ positions were most important for substrate specificity (55). We expressed and isolated PsAarA from *E. coli* (supplemental Fig. S1) as described previously (29) and incubated it with the 228-member peptide library for 0.25, 1, 4, and 20 h. In total, cleavage products from 29 hydrolyzed peptide bonds were identified and progress curves were generated. The rate constants were calculated to range from 1.04×10^3 $M^{-1}s^{-1}$ to 1.47×10^{-1} $M^{-1}s^{-1}$ (Fig. 3*A*). PsAarA frequently cleaved at sites that have small aliphatic amino acids in the P1 position and bulky hydrophobic amino acids such as Phe in the P2′ and P4 positions. In addition, Leu was frequently found in the P2 position whereas Arg and Ser were present in P1′ (Fig. 3*B*). Although we were only able to quantify a low number of cleavage products, the overall substrate preference is like the substrate preference previously reported by Strisovsky and colleagues (55).

We next assayed a rhomboid peptidase from *Haemophilus influenzae* (HiGlpG) that had not previously been characterized for substrate specificity. This enzyme was also expressed and purified from *E. coli* however only two substrates were hydrolyzed following 20 h of incubation with the peptide mixture. The k_{cat}/K_m values for PQnIGHVKLFRFN*W and KWLIHPTF*SYnRWP were calculated to be 8.97×10^3 $M^{-1}s^{-1}$ and 5.61×10^3 $M^{-1}s^{-1}$, respectively, where * indicates the cleavage site. Interestingly, although the substrate preference of HiGlpG is more stringent than PsAarA, PQnIGHVKLFRFN*W was the most efficiently hydrolyzed substrate for both enzymes. This substrate likely contains sequence features that promote favorable interaction with the enzyme active site that is buried within the detergent

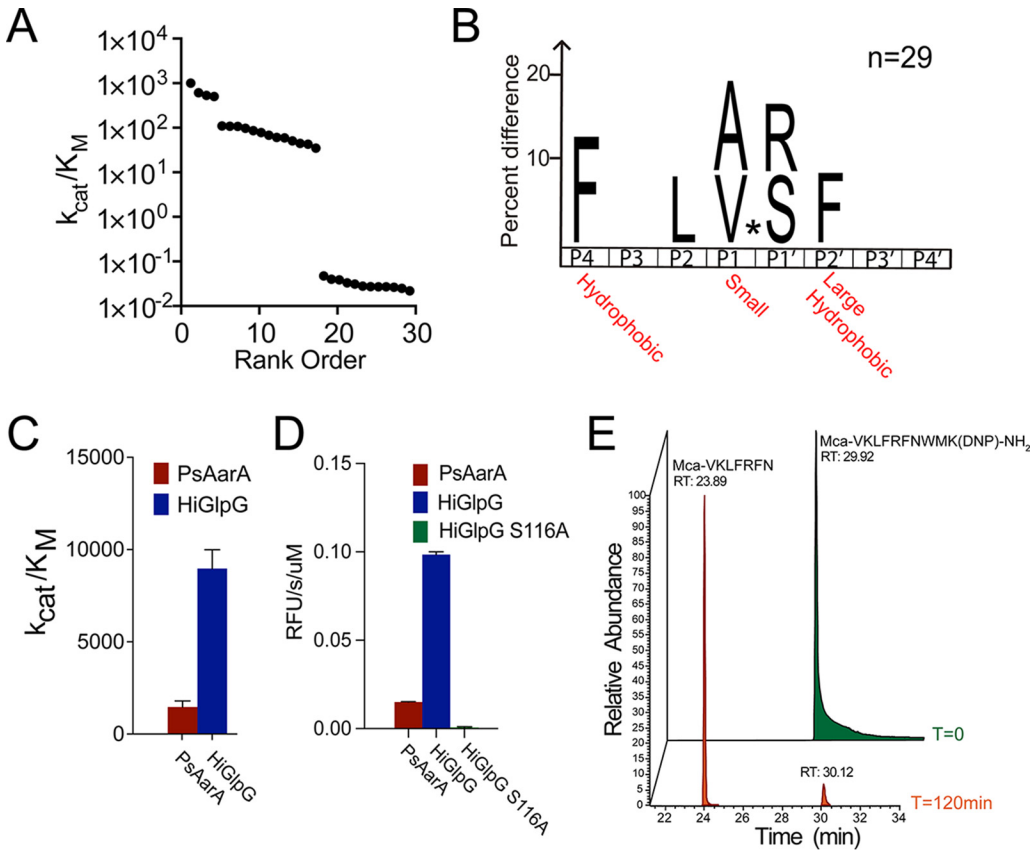

FIG. 3. **Substrate specificities and fluorescent assays of rhomboid peptidases.** *A*, Proteolytic constant k_{cat}/K_m of each cleaved peptide was calculated and ranked. *B*, PsAarA specificity profile was generated using 29 cleavages ($p < 0.05$). Because of the low number of cleavage sites, no amino acid was found to be significantly de-enriched. Text in red was previously described to be the specificity of PsAarA (55). *C*, PQnIGHVKLFRFNW was cleaved by PsAarA and HiGlpG between Asn and Trp and cleavage efficiencies were calculated. *D*, Fluorescent substrate screening of PsAarA, HiGlpG and HiGlpG S116A with the rationally designed internally quenched substrate IQ1. *E*, Cleavage of the fluorescent substrate between Asn and Trp was confirmed by mass spectrometry.

micelle. A peptide corresponding to the P7 to P1′ amino acids (VKLFRFN*W) was synthesized flanked on the N terminus with a fluorescent reporter molecule, 7-methoxycoumarin-4-acetic acid and on the C terminus a quenching group, 2,4-dinitrophenol (supplemental Table S4). This soluble fluorescent substrate was then assayed with HiGlpG and PsAarA and the rate of cleavage was determined in a microplate assay. In the qMSP-MS assay, HiGlpG cleaved the 14-mer peptide substrate six times faster than PsAarA (Fig. 3*C*). This rate difference was also seen for the fluorescent substrate (Fig. 3*D*). In addition, we assayed a catalytically inactive HiGlpG, consisting of a Ser to Ala mutation at position 116, with the fluorescent substrate and failed to detect hydrolysis. This mutant protein was expressed and purified under identical conditions to the active enzyme, thereby providing a control sample to ensure that proteolytic activity associated with this wild-type enzyme was not because of a contaminating *E. coli* peptidase. Finally, we sequenced the cleavage products of the fluorescent substrate and determined that hydrolysis occurred between Asn and Trp confirming that addition of the fluorophore and quencher molecules does not affect the cleavage site specificity of this substrate (Fig. 3*E*, supplemental Fig. S2). Taken together, these studies revealed that HiGlpG has narrow specificity but higher catalytic activity than PsAarA.

Characterization of Proteolytic Activities of a Complex Peptidase Sample—We next investigated the use of the qMSP-MS assay for characterizing complex biological samples containing peptidases from diverse families. Using a commercial extract from *Aspergillus phoenicis* that is known to contain α-galactosidase and 1,3-β-D-glucanse activities (56, 57) we confirmed by SDS-PAGE and proteomics that this sample contained many fungal proteins (supplemental Fig. S3). In total we identified 528 proteins of which, 49 were peptidases that could be classified into 4 families, namely, serine-, cysteine-, aspartyl and metallopeptidases (Fig. 4*A*). Serine peptidases were the most frequently found proteolytic enzymes in the extract whereas cysteine peptidases were the least frequent. However, by spectral counting, aspartyl peptidases were the most abundant proteolytic enzymes found (Fig. 4*A*). We assayed this sample at pH 5.0 with the synthetic peptide library and quantified 243 cleaved products. As the

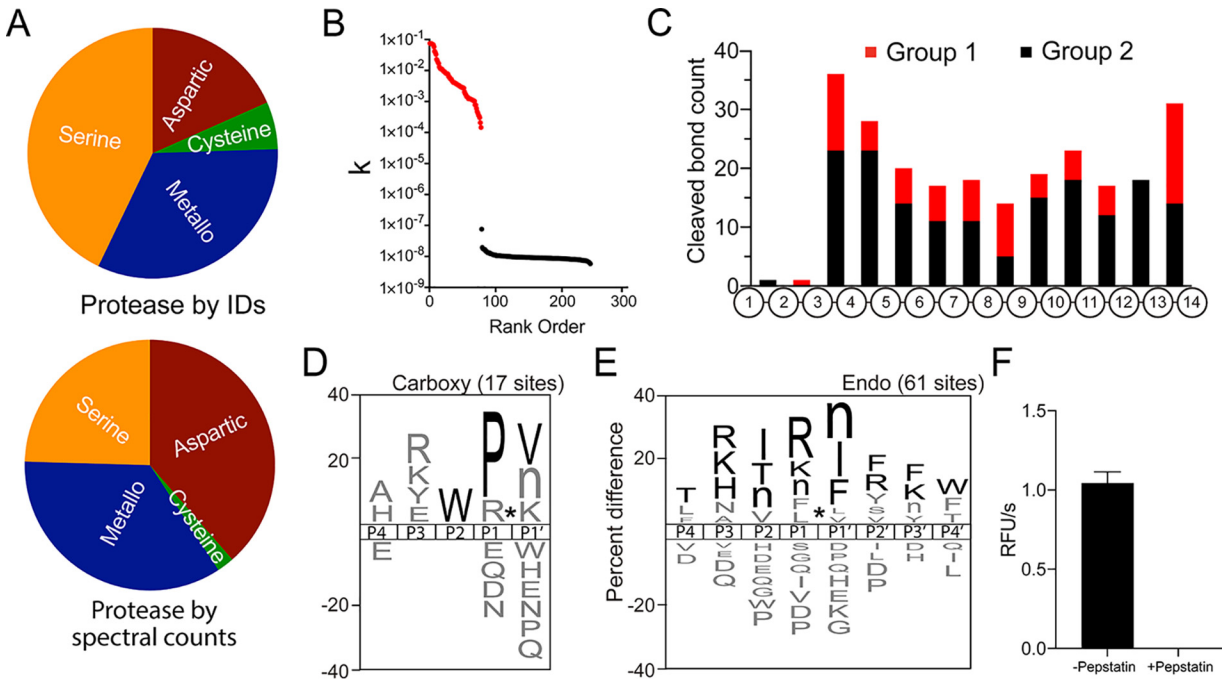

FIG. 4. **Proteomic analysis and Quantitative multiplex substrate profiling of *Aspergillus phoenicis* (*Aspph*) extract.** *A*, Proteomic analysis of *Aspph* extract revealed the presence of 51 proteases. Spectral counts ranking determined that aspartyl peptidases were abundant in *Aspph* extract. *B*, Proteolytic efficiency, $k = k_{cat}/K_m \times [E_0]$, for 243 cleavage products were calculated, ranked, and clustered into Group 1 (red) and Group 2 (black). *C*, Distribution of Group 1 and 2 cleavage sites within 14-mer peptides. *D*, Substrate specificity profile of mono-carboxypeptidase activities. Lowercase "n" corresponds to norleucine and nongrayed residues have $p < 0.05$. Cleavage sites are indicated with *. *E*, Substrate specificity profile of endopeptidases activities. *F*, *Aspph* extract cleaved fluorescent substrate IQ2 and the activity is completely inhibited with addition of pepstatin.

concentration of each peptidase within this sample is unknown, proteolytic efficiencies of each cleavage were calculated as k values where $k = k_{cat}/K_m \times [E_0]$ and clustered into two groups (Fig. 4*B*). Peptidases in this extract rarely cleaved bonds between amino acids 1 and 3 indicting that no aminopeptidases were active under these assay conditions. In addition, cleavage of the peptide bonds between position 12 and 13 was slow and only found in Group 2. These data indicate that acid-acting endopeptidases rapidly hydrolyze peptide bonds between position 3 and 12 whereas one or more acid-acting carboxypeptidase cleaves single amino acids from the C terminus of these peptides (Fig. 4*C*).

We generated a specificity profile of the carboxypeptidase activity and found that these enzymes in the fungal extract remove C-terminal Val, Nle and Lys when Pro or Arg are in the penultimate position and Trp is in the P2 position (Fig. 4*D*). The cleavage profile of the endopeptidases showed a preference for hydrophobic and positively charged amino acids in the P1 positions and whereas hydrophobic amino acids were exclusively found in the P1′ position. In addition, positively charged amino acids were frequently present in the P3 position (Fig. 4*E*). This substrate profile was like the cleavage specificity generated by secreted aspartyl peptidases from *Malassezia glabosa* (48) and *Candida albicans* (58). Therefore, we assayed the *Aspph* extract with a fluorescent substrate IQ2 (supplemental Table S4) used for aspartic acid peptidases (59) and found that it was efficiently hydrolyzed. Cleavage occurred between the Phe-Phe bond (supplemental Fig. S4) and this activity was completely inhibited by pepstatin, an aspartyl peptidase inhibitor (Fig. 4*F*).

These studies show that the qMSP-MS assay can be used to distinguish between endo- and exo-peptidases within complex biological samples. In addition, knowledge of peptidase class and understanding of the cleavage pattern facilitated the identification of fluorescent reporter substrates that can be used for subsequent biochemical assays.

Application of qMSP-MS in Studying Lung Cancer Pericellular Peptidase Activities—In-depth transcriptional analysis of cell lines and tumors has identified candidate peptidases that may play a role in disease progression. However, such expression-based strategies to study peptidases cannot account for the effects of translational regulation, post-translational modifications, stability and the presence of endogenous inhibitors in the pericellular environment. Therefore, increased expression of a peptidase may not result in a concomitant increase in proteolytic activity. New, function-based technologies with high information content are needed to detect dysregulated proteolysis in the tumor microenvironment. Given that we have demonstrated qMSP-MS can be used to uncover the proteolytic activity in complex protein samples mixture, we sought to apply this method to study the secreted peptidase activity from a panel of cell lines representing four

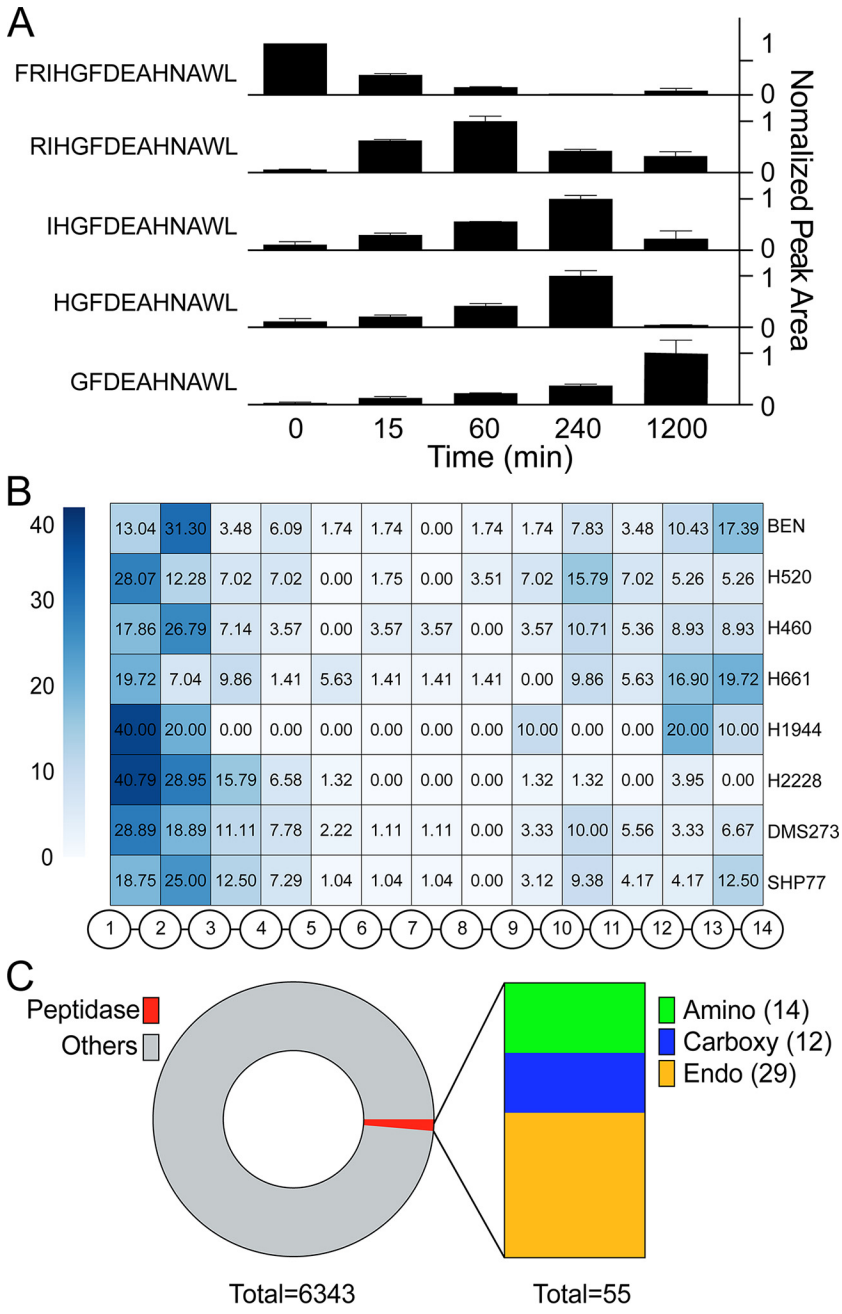

FIG. 5. **Application of qMSP-MS to lung cancer secretions.** *A*, An example showing the N terminus of a substrate being sequentially cleaved by aminopeptidases in DMS273 secretion. *B*, Analysis of cleavage loci within the tetradecapeptide library. Numbers represent the percentage of cleavage sites at each position relative to the total cleavage sites generated by secreted peptidases in each cell line. *C*, 55 peptidases identified in lung cancer secretions of which 14 are predicted to be aminopeptidases and 12 are predicted to be carboxypeptidases.

sub-types of lung cancer (supplemental Table S1). The long-term goal is to identify key peptidase activities that can be targeted in the tumor microenvironment for diagnostics, imaging, or prodrug activation.

Using qMSP-MS, we characterized the secreted proteolytic activity in conditioned media from these lung cancer cell lines. However, unlike previous assays with papain and *Aspergillus phoenicis* extract, we found that most peptides were sequentially hydrolyzed at the amino and C terminus and the initial cleavage products were subsequently degraded at later time points. For example, the substrate FRIHGFDEAHNAWL was hydrolyzed to GFDEAHNAWL by sequential removal of F, R, I, and H from the N terminus by peptidases secreted from DMS273 cells (Fig 5*A*). Therefore, the progression curve of each cleavage product was not monotonic and therefore did not conform to pseudo-first order kinetics. To address this issue, we calculated the change in abundance of each cleavage product between two time intervals (supplemental Fig. S5). Our results showed that most cleavage events occurred at the N terminus of the tetradecapeptides, indicating the presence of strong aminopeptidases activities in lung cancer secretions (Fig. 5*B*). In addition, BEN, H661, H1944, and SHP77 secrete peptidases with a preference for removing single amino acids from the C terminus of the tetrapeptides. In

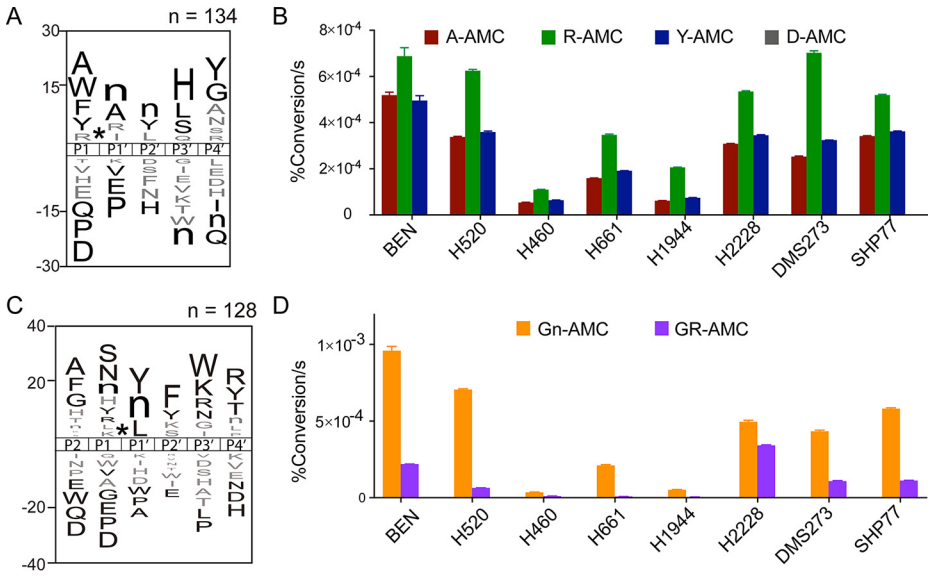

FIG. 6. **Global specificity profiles of aminopeptidases activities in lung cancer secretions and fluorescent substrate screenings.** *A*, qMSP-MS showed the specificity profile of mono-aminopeptidases activities using the pool of cleavages from all lung cancer secretions. Lowercase "n" corresponds to norleucine and nongrayed residues have $p < 0.05$. Cleavage sites are indicated with *. *B*, Mono-amino fluorescent substrates were designed based on the profiles for orthogonal validation. *C*, qMSP-MS showed the specificity profile of di-aminopeptidases activities using the pool of cleavages from all lung cancer secretions. *D*, Di-amino fluorescent substrates were designed based on the profiles for orthogonal validation. Data presented as mean ± sd of triplicate assays.

parallel, quantitative shotgun proteomics of secretions from each of the cell lines was performed to identify peptidases that were present in the conditioned media. In total, 6343 unique proteins were identified, 55 of which were peptidases, including 14 aminopeptidases, 12 carboxypeptidases and 29 endopeptidases (Fig. 5*C*). The qMSP-MS assay data clearly indicated that aminopeptidases were more active than the endopeptidases and carboxypeptidases in these lung cancer secretions and therefore we focused on developing fluorescent substrates to further characterize the amino peptidase activities.

We generated substrate specificity profiles of proteolysis between residue 1 and 2 corresponding to mono-aminopeptidases activity for all cell lines (Fig. 6*A*) and discovered that these human aminopeptidases frequently removed Ala, Trp, Phe, Tyr and Arg from the N terminus whereas rarely or never cleaving Asp, Pro and Gln. We subsequently evaluated a selection of mono-aminopeptidase substrates consisting of Ala, Tyr and Arg linked to the fluorescent reporter molecule, 7-amino-4-methylcoumarin (AMC). These substrates were hydrolyzed by aminopeptidases in conditioned media from all cell lines (Fig. 6*B*). The rate of cleavage of Ala-AMC and Tyr-AMC was similar in all cell lines whereas hydrolysis of Arg-AMC was generally 1.5 to 3-fold faster. In the substrate profiling assay, tetradecapeptides with N-terminal Asp are rarely hydrolyzed. Therefore, we designed Asp-AMC as a negative control to assay these secretions and found there was no detectable cleavage of this substrate.

In some tetradecapeptide substrates, removal of two amino acids from the N terminus was commonly observed. In most cases, this appears to be because of di-aminopeptidase activity rather than two sequential mono-aminopeptidase cleavage events because some 12-mer cleavage products were found but not the related 13-mer intermediate product. In addition, we cannot rule out that these substrates are also cleaved by endopeptidases that have little or no specificity beyond the P2 position. We generated a substrate specificity profile of peptide cleavage sites between residue 2 and 3 (Fig. 6*C*). From this specificity profile, we designed two dipeptide substrates that are unlikely to be hydrolyzed by mono-aminopeptidases. To achieve this, we included a terminal Gly residue because this amino acid is significantly enriched in the P2 position but not preferentially cleaved by mono-aminopeptidases. In the P1 position, we included Nle or Arg, two amino acids that are frequently enriched in the substrate profile. The results showed that both fluorescent substrates were commonly hydrolyzed by lung cancer cell secretions but at different rates (Fig. 6*D*). In addition, H460, H661 and H1944 cell secretions had reduced specific activity for both mono- and di-amino fluorescent substrates, indicating the aminopeptidases composition in these cell secretions might be lower compared with the others. Taken together, the fluorescent substrate screening assays supported the qMSP-MS specificity profile and demonstrates that this assay is not limited to characterizing purified peptidases but can be applied to studying complex biological samples. The specificity information generated from these lung cancer cell lines will be used for developing activity-based diagnostics or prodrugs that will be activated in the tumor microenvironment by one or more peptidases.

DISCUSSION

Several studies have used isobaric labels to quantify peptides that are modified by proteolysis, phosphorylation, or methylation (60–66). These labels are generally used to directly compare the peptide abundance between multiple biological samples or within a single biological sample that has been subjected to different treatment regimes. In this study, we use isobaric labels to quantify and rank hundreds of peptide cleavage reactions that take place simultaneously. Pre-

viously, we developed a library of 124 tetradecapeptides composed of all neighbor and near-neighbor amino acid pairs and monitored the time dependent appearance of cleavage products on addition of a peptidase (19). This method used tandem mass spectrometry to identify new products but like many other substrate profiling methods (10, 14), it was largely qualitative. We therefore incorporated TMT labels into our MSP-MS workflow to minimize experimental and instrumentation derived variance while improving throughput of the assay. More importantly, by labeling samples at multiple time intervals, we were able to perform accurate quantification of peptides, allowing us to calculate the turnover rate of each proteolytic event.

To validate our workflow, we demonstrated that qMSP-MS can accurately characterize papain substrate specificity. We highlighted the necessity of calculating the cleavage efficiency of different peptides as it can vary by eight orders of magnitude. This information is crucial when studying peptidases as it allows us to identify individual amino acids within the substrate sequence that promote rapid hydrolysis of the peptide. Previously, papain was found to preferentially cleave many hydrophobic amino acids at the P2 position (51, 52). However, we demonstrated that Val, Ile, Ala, and Leu are strongly favored over other hydrophobic amino acids such as Tyr, Nle, Phe, and Pro.

To further demonstrate the versatility of this method, we assayed two related intramembrane peptidases whose active sites are buried in the lipid bilayer of cell membranes. It is unknown how many of the 228 peptides can access the active site and therefore substrate specificity may be influenced by sequence features of the peptide that promote or prevent accessibility to the active site. Using qMSP-MS, we found that HiGlpG has stricter specificity and higher catalytic activity than PsAarA and a single fluorescent substrate was designed that could monitor activity of both enzymes. Compared with the standard gel-based methods for detecting rhomboid protease activity (55, 67), this fluorescent substrate can be used in microplate assays and therefore facilitates rapid and quantitative activity assays for integral membrane peptidases. Five members of this rhomboid peptidase family are found in mammalian cells and these enzymes are associated with tumor metastasis, tumor angiogenesis, type 2 diabetes and neurodegenerative disorders (68). In general, these integral membrane serine peptidases are much less characterized than their soluble serine peptidase counterparts and no substrates have been discovered for RHBDL1 and RHBDL3. Therefore, quantitative substrate specificity technologies like qMSP-MS can be used to uncover the substrate specificity of these enzymes, facilitating the discovery of their biological substrates.

From these findings, we predicted that qMSP-MS would have an impact on designing substrates for monitoring proteolytic activities and developing peptidase-activated drugs where potency and selectivity are essential. The qMSP-MS assay can pinpoint which sequences are preferred by peptidases, allowing us to design optimal substrates for peptidase screening. Our studies on the *Aspph* extract mixture showed the power of qMSP-MS in studying complex samples and designing individual fluorescent substrates that can be used to monitor their activities. As a final evaluation of qMSP-MS performance in the context of a complex peptidase system, we applied it to a panel of lung cancer cell line secretions, representing the first global characterization and comparison of proteolytic activity in the cancer pericellular environment.

Lung cancer represents 25% of all cancer diagnoses, corresponding to 200,000 new cases in the United States each year. Further, it is the second most deadly cancer with only an 18% 5-year survival rate (58). Increased pericellular proteolysis is a hallmark of aggressive cancers (59). Secreted peptidases can modulate tumor progression and metastasis through highly regulated processes that involve shedding of cell adhesion molecules and processing of growth factors and cytokines (60–65). Various strategies have been developed to use peptidases for drug delivery for cancer chemotherapy (69, 70) and surgery (71). Traditionally, the discovery of peptidase targets for prodrugs or antibody-drug conjugate activation is largely on the expression level and further downstream characterizations are usually required. However, our qMSP-MS method allows us to functionally characterize peptidases specificities, which narrows the gap between biological discovery and drug design, offering valuable information for translational studies. In this study, we showed the application of qMSP-MS to this panel of lung cancer cell lines, demonstrating the feasibility of this approach for studying dynamic diseases.

Aminopeptidase activity has previously been detected in blood (63) and inflamed skin (72) using N-terminal enrichment strategies, whereas carboxypeptidase activity has been detected in mammalian (73) and bacterial (74) cell lysates using C-terminal enrichment strategies. In the lung cancer secretions, we detected both N-terminal and C-terminal trimming of many peptide substrates that we predict are the result of aminopeptidase and carboxypeptidase activity. In addition, we developed a panel of fluorescent substrates to quantify mono- and di-aminopeptidase activity in microplate assays. Our findings, together with previous studies, indicated that aminopeptidases and carboxypeptidases are associated with tumor invasion and metastasis, but the development of exopeptidase inhibitors for cancer treatment is in a relatively early stage (75–78). The logical next step from the outcomes of our study would be to design peptidase-activated prodrugs targeted to global pericellular proteolysis in tumor microenvironment. As MS technology and multiplexing abilities continue to advance, driving down costs and instrumentation time requirements, it is easy to foresee qMSP-MS as a potential first step in the development of personalized medicine geared toward not only tumors, but other peptidase-related diseases as well.

Acknowledgments—We thank Dr. Philippe Montgrain (UCSD) and Dr. Edward D. Ball (UCSD) for providing lung cancer cell lines.

DATA AVAILABILITY

All mass spectrometry data have been deposited in MassIVE and proteomeXchange with accession numbers: MassIVE: MSV000082187; ProteomeXchange: PXD009269.

* A.J.O. and D.J.G. gratefully acknowledge financial support from UC San Diego Skaggs School of Pharmacy and Pharmaceutical Science. A.J.O was supported by an American Cancer Society Institutional Research Grant #14-250-42 provided through the Moores Cancer Center, University of California, San Diego. D.J.G. was supported by the Ray Thomas Edwards Foundation and the University of California Office of the President. J.D.L. is an IRACDA fellow supported by NIGMS/NIH (K12GM068524). J.M.W. was supported by Graduate Training in Cellular and Molecular Pharmacology Training Grant NIH T32 GM007752. Z.J. is supported by Chancellor's Research Excellence Scholarships from UC San Diego. M.J.L acknowledges support from the Canadian Institute of Health Research, Brad Mates E Drive Research Fund and Parkinson Alberta.

This article contains supplemental material.

§§ To whom correspondence may be addressed. E-mail: djgonzalez@ucsd.edu.

¶¶ To whom correspondence may be addressed. E-mail: ajodonoghue@ucsd.edu.

‡‡ Authors contributed equally to this work.

Author contributions: J.D.L., Z.J., D.J.G., and A.J.O. designed research; J.D.L., Z.J., J.M.W., and S.C.W. performed research; J.D.L., Z.J., and J.M.W. analyzed data; J.D.L., Z.J., J.M.W., E.A., S.C.W., M.J.L., D.J.G., and A.J.O. wrote the paper; E.A. and M.J.L. provided the membrane peptidases.

REFERENCES

1. Rawlings, N. D., and Salvesen, G. (2013) *Handbook of proteolytic enzymes*. 3rd Ed., Academic Press, London; Boston
2. Turk, B. (2006) Targeting proteases: successes, failures and future prospects. *Nat. Rev. Drug Discov.* **5,** 785–799
3. Choi, K. Y., Swierczewska, M., Lee, S., and Chen, X. (2012) Protease-activated drug development. *Theranostics* **2,** 156–178
4. Harris, J. L., Backes, B. J., Leonetti, F., Mahrus, S., Ellman, J. A., and Craik, C. S. (2000) Rapid and general profiling of protease specificity by using combinatorial fluorogenic substrate libraries. *Proc. Natl. Acad. Sci. U.S.A.* **97,** 7754–7759
5. Poreba, M., Kasperkiewicz, P., Snipas, S. J., Fasci, D., Salvesen, G. S., and Drag, M. (2014) Unnatural amino acids increase sensitivity and provide for the design of highly selective caspase substrates. *Cell Death Differ.* **21,** 1482–1492
6. Wysocka, M., Lesner, A., Guzow, K., Mackiewicz, L., Legowska, A., Wiczk, W., and Rolka, K. (2008) Design of selective substrates of proteinase 3 using combinatorial chemistry methods. *Anal. Biochem.* **378,** 208–215
7. Oliveira, L. C., Silva, V. O., Okamoto, D. N., Kondo, M. Y., Santos, S. M., Hirata, I. Y., Vallim, M. A., Pascon, R. C., Gouvea, I. E., Juliano, M. A., and Juliano, L. (2012) Internally quenched fluorescent peptide libraries with randomized sequences designed to detect endopeptidases. *Anal. Biochem.* **421,** 299–307
8. Boulware, K. T., and Daugherty, P. S. (2006) Protease specificity determination by using cellular libraries of peptide substrates (CLiPS). *Proc. Natl. Acad. Sci. U.S.A.* **103,** 7583–7588
9. Matthews, D. J., and Wells, J. A. (1993) Substrate phage: selection of protease substrates by monovalent phage display. *Science* **260,** 1113–1117
10. Schilling, O., and Overall, C. M. (2008) Proteome-derived, database-searchable peptide libraries for identifying protease cleavage sites. *Nat. Biotechnol.* **26,** 685–694
11. Kleifeld, O., Doucet, A., auf dem Keller, U., Prudova, A., Schilling, O., Kainthan, R. K., Starr, A. E., Foster, L. J., Kizhakkedathu, J. N., and Overall, C. M. (2010) Isotopic labeling of terminal amines in complex samples identifies protein N-termini and protease cleavage products. *Nat. Biotechnol.* **28,** 281–288
12. Gevaert, K., Goethals, M., Martens, L., Van Damme, J., Staes, A., Thomas, G. R., and Vandekerckhove, J. (2003) Exploring proteomes and analyzing protein processing by mass spectrometric identification of sorted N-terminal peptides. *Nat. Biotechnol.* **21,** 566–569
13. Mahrus, S., Trinidad, J. C., Barkan, D. T., Sali, A., Burlingame, A. L., and Wells, J. A. (2008) Global sequencing of proteolytic cleavage sites in apoptosis by specific labeling of protein N termini. *Cell* **134,** 866–876
14. Vizovisek, M., Vidmar, R., and Fonovic, M. (2017) FPPS: Fast Profiling of Protease Specificity. *Methods Mol. Biol.* **1574,** 183–195
15. Staes, A., Impens, F., Van Damme, P., Ruttens, B., Goethals, M., Demol, H., Timmerman, E., Vandekerckhove, J., and Gevaert, K. (2011) Selecting protein N-terminal peptides by combined fractional diagonal chromatography. *Nat. Protoc.* **6,** 1130–1141
16. Kleifeld, O., Doucet, A., Prudova, A., auf dem Keller, U., Gioia, M., Kizhakkedathu, J. N., and Overall, C. M. (2011) Identifying and quantifying proteolytic events and the natural N terminome by terminal amine isotopic labeling of substrates. *Nat. Protoc.* **6,** 1578–1611
17. Thornberry, N. A., Rano, T. A., Peterson, E. P., Rasper, D. M., Timkey, T., Garcia-Calvo, M., Houtzager, V. M., Nordstrom, P. A., Roy, S., Vaillancourt, J. P., Chapman, K. T., and Nicholson, D. W. (1997) A combinatorial approach defines specificities of members of the caspase family and granzyme B. Functional relationships established for key mediators of apoptosis. *J. Biol. Chem.* **272,** 17907–17911
18. Backes, B. J., Harris, J. L., Leonetti, F., Craik, C. S., and Ellman, J. A. (2000) Synthesis of positional-scanning libraries of fluorogenic peptide substrates to define the extended substrate specificity of plasmin and thrombin. *Nat. Biotechnol.* **18,** 187–193
19. O'Donoghue, A. J., Eroy-Reveles, A. A., Knudsen, G. M., Ingram, J., Zhou, M., Statnekov, J. B., Greninger, A. L., Hostetter, D. R., Qu, G., Maltby, D. A., Anderson, M. O., Derisi, J. L., McKerrow, J. H., Burlingame, A. L., and Craik, C. S. (2012) Global identification of peptidase specificity by multiplex substrate profiling. *Nat. Methods* **9,** 1095–1100
20. O'Donoghue, A. J., Knudsen, G. M., Beekman, C., Perry, J. A., Johnson, A. D., DeRisi, J. L., Craik, C. S., and Bennett, R. J. (2015) Destructin-1 is a collagen-degrading endopeptidase secreted by Pseudogymnoascus destructans, the causative agent of white-nose syndrome. *Proc. Natl. Acad. Sci. U.S.A.* **112,** 7478–7483
21. Winter, M. B., La Greca, F., Arastu-Kapur, S., Caiazza, F., Cimermancic, P., Buchholz, T. J., Anderl, J. L., Ravalin, M., Bohn, M. F., Sali, A., O'Donoghue, A. J., and Craik, C. S. (2017) Immunoproteasome functions explained by divergence in cleavage specificity and regulation. *Elife* **6,** e27364
22. Roncase, E. J., Moon, C., Chatterjee, S., Gonzalez-Paez, G. E., Craik, C. S., O'Donoghue, A. J., and Wolan, D. W. (2017) Substrate Profiling and High Resolution Co-complex Crystal Structure of a Secreted C11 Protease Conserved across Commensal Bacteria. *ACS Chem. Biol.* **12,** 1556–1565
23. Li, H., O'Donoghue, A. J., van der Linden, W. A., Xie, S. C., Yoo, E., Foe, I. T., Tilley, L., Craik, C. S., da Fonseca, P. C., and Bogyo, M. (2016) Structure- and function-based design of Plasmodium-selective proteasome inhibitors. *Nature* **530,** 233–236
24. Lentz, C. S., Ordonez, A. A., Kasperkiewicz, P., La Greca, F., O'Donoghue, A. J., Schulze, C. J., Powers, J. C., Craik, C. S., Drag, M., Jain, S. K., and Bogyo, M. (2016) Design of Selective Substrates and Activity-Based Probes for Hydrolase Important for Pathogenesis 1 (HIP1) from Mycobacterium tuberculosis. *ACS Infect. Dis.* **2,** 807–815
25. Joshi, S., Chen, L., Winter, M. B., Lin, Y. L., Yang, Y., Shapovalova, M., Smith, P. M., Liu, C., Li, F., and LeBeau, A. M. (2017) The Rational Design of Therapeutic Peptides for Aminopeptidase N using a Substrate-Based Approach. *Sci. Rep.* **7,** 1424
26. Ivry, S. L., Sharib, J. M., Dominguez, D. A., Roy, N., Hatcher, S. E., Yip-Schneider, M. T., Schmidt, C. M., Brand, R. E., Park, W. G., Hebrok, M., Kim, G. E., O'Donoghue, A. J., Kirkwood, K. S., and Craik, C. S. (2017) Global Protease Activity Profiling Provides Differential Diagnosis of Pancreatic Cysts. *Clin. Cancer Res.* **23,** 4865–4874
27. McAlister, G. C., Nusinow, D. P., Jedrychowski, M. P., Wuhr, M., Huttlin, E. L., Erickson, B. K., Rad, R., Haas, W., and Gygi, S. P. (2014) MultiNotch MS3 enables accurate, sensitive, and multiplexed detection of

differential expression across cancer cell line proteomes. *Anal. Chem.* **86,** 7150–7158
28. Thompson, A., Schafer, J., Kuhn, K., Kienle, S., Schwarz, J., Schmidt, G., Neumann, T., Johnstone, R., Mohammed, A. K., and Hamon, C. (2003) Tandem mass tags: a novel quantification strategy for comparative analysis of complex protein mixtures by MS/MS. *Anal. Chem.* **75,** 1895–1904
29. Arutyunova, E., Panwar, P., Skiba, P. M., Gale, N., Mak, M. W., and Lemieux, M. J. (2014) Allosteric regulation of rhomboid intramembrane proteolysis. *EMBO J.* **33,** 1869–1881
30. Villen, J., and Gygi, S. P. (2008) The SCX/IMAC enrichment approach for global phosphorylation analysis by mass spectrometry. *Nat. Protoc.* **3,** 1630–1638
31. Haas, W., Faherty, B. K., Gerber, S. A., Elias, J. E., Beausoleil, S. A., Bakalarski, C. E., Li, X., Villen, J., and Gygi, S. P. (2006) Optimization and use of peptide mass measurement accuracy in shotgun proteomics. *Mol. Cell. Proteomics* **5,** 1326–1337
32. Wessel, D., and Flugge, U. I. (1984) A method for the quantitative recovery of protein in dilute solution in the presence of detergents and lipids. *Anal. Biochem.* **138,** 141–143
33. Tolonen, A. C., and Haas, W. (2014) Quantitative proteomics using reductive dimethylation for stable isotope labeling. *J. Vis. Exp.* **89,** 51416
34. Wang, Y., Yang, F., Gritsenko, M. A., Wang, Y., Clauss, T., Liu, T., Shen, Y., Monroe, M. E., Lopez-Ferrer, D., Reno, T., Moore, R. J., Klemke, R. L., Camp, D. G., 2nd, and Smith, R. D. (2011) Reversed-phase chromatography with multiple fraction concatenation strategy for proteome profiling of human MCF10A cells. *Proteomics* **11,** 2019–2026
35. Lapek, J. D., Jr, Greninger, P., Morris, R., Amzallag, A., Pruteanu-Malinici, I., Benes, C. H., and Haas, W. (2017) Detection of dysregulated protein-association networks by high-throughput proteomics predicts cancer vulnerabilities. *Nat. Biotechnol.* **35,** 983–989
36. Lapek, J. D., Jr, Fang, R. H., Wei, X., Li, P., Wang, B., Zhang, L., and Gonzalez, D. J. (2017) Biomimetic virulomics for capture and identification of cell-type specific effector proteins. *ACS Nano* **11,** 11831–11838
37. Lapek, J. D., Jr, Lewinski, M. K., Wozniak, J. M., Guatelli, J., and Gonzalez, D. J. (2017) Quantitative temporal viromics of an inducible HIV-1 model yields insight to global host targets and phospho-dynamics associated with protein Vpr. *Mol. Cell. Proteomics* **16,** 1447–1461
38. Eng, J. K., McCormack, A. L., and Yates, J. R. (1994) An approach to correlate tandem mass spectral data of peptides with amino acid sequences in a protein database. *J. Am. Soc. Mass Spectrom.* **5,** 976–989
39. Elias, J. E., and Gygi, S. P. (2007) Target-decoy search strategy for increased confidence in large-scale protein identifications by mass spectrometry. *Nat. Methods* **4,** 207–214
40. Elias, J. E., Haas, W., Faherty, B. K., and Gygi, S. P. (2005) Comparative evaluation of mass spectrometry platforms used in large-scale proteomics investigations. *Nat. Methods* **2,** 667–675
41. Peng, J., Elias, J. E., Thoreen, C. C., Licklider, L. J., and Gygi, S. P. (2003) Evaluation of multidimensional chromatography coupled with tandem mass spectrometry (LC/LC-MS/MS) for large-scale protein analysis: the yeast proteome. *J. Proteome Res.* **2,** 43–50
42. Beausoleil, S. A., Villen, J., Gerber, S. A., Rush, J., and Gygi, S. P. (2006) A probability-based approach for high-throughput protein phosphorylation analysis and site localization. *Nat. Biotechnol.* **24,** 1285–1292
43. Huttlin, E. L., Jedrychowski, M. P., Elias, J. E., Goswami, T., Rad, R., Beausoleil, S. A., Villen, J., Haas, W., Sowa, M. E., and Gygi, S. P. (2010) A tissue-specific atlas of mouse protein phosphorylation and expression. *Cell* **143,** 1174–1189
44. Kall, L., Canterbury, J. D., Weston, J., Noble, W. S., and MacCoss, M. J. (2007) Semi-supervised learning for peptide identification from shotgun proteomics datasets. *Nat. Methods* **4,** 923–925
45. Spivak, M., Weston, J., Bottou, L., Kall, L., and Noble, W. S. (2009) Improvements to the percolator algorithm for Peptide identification from shotgun proteomics data sets. *J. Proteome Res.* **8,** 3737–3745
46. Rappsilber, J., Ishihama, Y., and Mann, M. (2003) Stop and go extraction tips for matrix-assisted laser desorption/ionization, nanoelectrospray, and LC/MS sample pretreatment in proteomics. *Anal. Chem.* **75,** 663–670
47. Colaert, N., Helsens, K., Martens, L., Vandekerckhove, J., and Gevaert, K. (2009) Improved visualization of protein consensus sequences by iceLogo. *Nat. Methods* **6,** 786–787
48. Li, H., Goh, B. N., Teh, W. K., Jiang, Z., Goh, J. P. Z., Goh, A., Wu, G., Hoon, S. S., Raida, M., Camattari, A., Yang, L., O'Donoghue, A. J., and Dawson, T. L., Jr. (2018) Skin Commensal Malassezia globosa secreted protease attenuates Staphylococcus aureus biofilm formation. *J. Invest. Dermatol.* **138,** 1137–1145
49. Bromme, D. (2001) Papain-like cysteine proteases. *Curr. Protoc. Protein Sci.* Chapter **21,** Unit 21.2
50. Fu, Y., Liu, J., Hansen, E. T., Bredie, W. L. P., and Lametsch, R. (2018) Structural characteristics of low bitter and high umami protein hydrolysates prepared from bovine muscle and porcine plasma. *Food Chem.* **257,** 163–171
51. Koga, H., Yamada, H., Nishimura, Y., Kato, K., and Imoto, T. (1990) Comparative study on specificities of rat cathepsin L and papain: amino acid differences at substrate-binding sites are involved in their specificities. *J. Biochem.* **108,** 976–982
52. Choe, Y., Leonetti, F., Greenbaum, D. C., Lecaille, F., Bogyo, M., Bromme, D., Ellman, J. A., and Craik, C. S. (2006) Substrate profiling of cysteine proteases using a combinatorial peptide library identifies functionally unique specificities. *J. Biol. Chem.* **281,** 12824–12832
53. Del Nery, E., Alves, L. C., Melo, R. L., Cesari, M. H., Juliano, L., and Juliano, M. A. (2000) Specificity of cathepsin B to fluorescent substrates containing benzyl side-chain-substituted amino acids at P1 subsite. *J. Protein Chem.* **19,** 33–38
54. Urban, S. (2016) A guide to the rhomboid protein superfamily in development and disease. *Semin. Cell Dev. Biol.* **60,** 1–4
55. Strisovsky, K., Sharpe, H. J., and Freeman, M. (2009) Sequence-specific intramembrane proteolysis: identification of a recognition motif in rhomboid substrates. *Mol. Cell* **36,** 1048–1059
56. Sugimoto, H., and Buren, J. P. (1970) v. Removal of oligosaccharides from soy milk by an enzyme from Aspergillus saitoi. *J. Food Sci.* 35, 655–660
57. Kasahara, S., Nakajima, T., Miyamoto, C., Wada, K., Furuichi, Y., and Ichishima, E. (1992) Characterization and mode of action of exo-1,3-β-d-glucanase from Aspergillus saitoi. *J. Fermentation Bioengineering* **74,** 238–240
58. Winter, M. B., Salcedo, E. C., Lohse, M. B., Hartooni, N., Gulati, M., Sanchez, H., Takagi, J., Hube, B., Andes, D. R., Johnson, A. D., Craik, C. S., and Nobile, C. J. (2016) Global identification of biofilm-specific proteolysis in Candida albicans. *MBio* **7,** e01514-16
59. Farzan, M., Schnitzler, C. E., Vasilieva, N., Leung, D., and Choe, H. (2000) BACE2, a beta -secretase homolog, cleaves at the beta site and within the amyloid-beta region of the amyloid-beta precursor protein. *Proc. Natl. Acad. Sci. U.S.A.* **97,** 9712–9717
60. Jakoby, T., van den Berg, B. H., and Tholey, A. (2012) Quantitative protease cleavage site profiling using tandem-mass-tag labeling and LC-MALDI-TOF/TOF MS/MS analysis. *J. Proteome Res.* **11,** 1812–1820
61. Shishkova, E., Zeng, H., Liu, F., Kwiecien, N. W., Hebert, A. S., Coon, J. J., and Xu, W. (2017) Global mapping of CARM1 substrates defines enzyme specificity and substrate recognition. *Nat. Commun.* **8,** 15571
62. Trinidad, J. C., Thalhammer, A., Specht, C. G., Lynn, A. J., Baker, P. R., Schoepfer, R., and Burlingame, A. L. (2008) Quantitative analysis of synaptic phosphorylation and protein expression. *Mol. Cell. Proteomics* **7,** 684–696
63. Wildes, D., and Wells, J. A. (2010) Sampling the N-terminal proteome of human blood. *Proc. Natl. Acad. Sci. U.S.A.* **107,** 4561–4566
64. Schlage, P., Egli, F. E., Nanni, P., Wang, L. W., Kizhakkedathu, J. N., Apte, S. S., and auf dem Keller, U. (2014) Time-resolved analysis of the matrix metalloproteinase 10 substrate degradome. *Mol. Cell. Proteomics* **13,** 580–593
65. Schlage, P., Kockmann, T., Sabino, F., Kizhakkedathu, J. N., and Auf dem Keller, U. (2015) Matrix metalloproteinase 10 degradomics in keratinocytes and epidermal tissue identifies bioactive substrates with pleiotropic functions. *Mol. Cell. Proteomics* **14,** 3234–3246
66. Plasman, K., Van Damme, P., Kaiserman, D., Impens, F., Demeyer, K., Helsens, K., Goethals, M., Bird, P. I., Vandekerckhove, J., and Gevaert, K. (2011) Probing the efficiency of proteolytic events by positional proteomics. *Mol. Cell. Proteomics* **10,** M110.003301
67. Urban, S., and Freeman, M. (2003) Substrate specificity of rhomboid intramembrane proteases is governed by helix-breaking residues in the substrate transmembrane domain. *Mol. Cell* **11,** 1425–1434
68. Dusterhoft, S., Kunzel, U., and Freeman, M. (2017) Rhomboid proteases in human disease: Mechanisms and future prospects. *Biochim. Biophys. Acta* **1864,** 2200–2209

69. Zhong, Y. J., Shao, L. H., and Li, Y. (2013) Cathepsin B-cleavable doxorubicin prodrugs for targeted cancer therapy (Review). *Int. J. Oncol.* **42,** 373–383
70. Vartak, D. G., and Gemeinhart, R. A. (2007) Matrix metalloproteases: underutilized targets for drug delivery. *J. Drug Target* **15,** 1–20
71. Nguyen, Q. T., Olson, E. S., Aguilera, T. A., Jiang, T., Scadeng, M., Ellies, L. G., and Tsien, R. Y. (2010) Surgery with molecular fluorescence imaging using activatable cell-penetrating peptides decreases residual cancer and improves survival. *Proc. Natl. Acad. Sci. U.S.A.* **107,** 4317–4322
72. auf dem Keller, U., Prudova, A., Eckhard, U., Fingleton, B., and Overall, C. M. (2013) Systems-level analysis of proteolytic events in increased vascular permeability and complement activation in skin inflammation. *Sci. Signal* **6,** rs2
73. Tanco, S., Lorenzo, J., Garcia-Pardo, J., Degroeve, S., Martens, L., Aviles, F. X., Gevaert, K., and Van Damme, P. (2013) Proteome-derived peptide libraries to study the substrate specificity profiles of carboxypeptidases. *Mol. Cell. Proteomics* **12,** 2096–2110
74. Schilling, O., Barre, O., Huesgen, P. F., and Overall, C. M. (2010) Proteome-wide analysis of protein carboxy termini: C terminomics. *Nat. Methods* **7,** 508–511
75. Wickstrom, M., Larsson, R., Nygren, P., and Gullbo, J. (2011) Aminopeptidase N (CD13) as a target for cancer chemotherapy. *Cancer Sci.* **102,** 501–508
76. Hitzerd, S. M., Verbrugge, S. E., Ossenkoppele, G., Jansen, G., and Peters, G. J. (2014) Positioning of aminopeptidase inhibitors in next generation cancer therapy. *Amino Acids* **46,** 793–808
77. Tokuhara, T., Hattori, N., Ishida, H., Hirai, T., Higashiyama, M., Kodama, K., and Miyake, M. (2006) Clinical significance of aminopeptidase N in nonsmall cell lung cancer. *Clin. Cancer Res.* **12,** 3971–3978
78. Novakova, Z., Cerny, J., Choy, C. J., Nedrow, J. R., Choi, J. K., Lubkowski, J., Berkman, C. E., and Barinka, C. (2016) Design of composite inhibitors targeting glutamate carboxypeptidase II: the importance of effector functionalities. *FEBS J.* **283,** 130–143